Purification and biochemical characterization of the D6 chemokine receptor

Paul E. BLACKBURN*†, Clare V. SIMPSON*†, Robert J. B. NIBBS*‡, Maureen O'HARA*†, Rhona BOOTH*†, Jemma POULOS*†, Neil W. ISAACS†[1] and Gerard J. GRAHAM*‡[1]

*The Beatson Institute for Cancer Research, Cancer Research U.K. Beatson Laboratories, Garscube Estate, Switchback Road, Bearsden, Glasgow G61 1BD, U.K., †Department of Chemistry, University of Glasgow, Glasgow G12 8QQ, U.K., and ‡Division of Immunity, Infection and Inflammation, University of Glasgow, Glasgow G12 8QQ, U.K.

There is much interest in chemokine receptors as therapeutic targets in diseases such as AIDS, autoimmune and inflammatory disorders, and cancer. Hampering such studies is the lack of accurate three-dimensional structural models of these molecules. The CC-chemokine receptor D6 is expressed at exceptionally high levels in heterologous transfectants. Here we report the purification and biochemical characterization of milligram quantities of D6 protein from relatively small cultures of transfected mammalian cells. Importantly, purified D6 retains full functional activity, shown by displaceable binding of ^{125}I-labelled MIP-1β (macrophage inflammatory protein-1β) and by complete binding of the receptor to a MIP-1α affinity column. In addition, we show that D6 is decorated on the N-terminus by N-linked glycosylation. Mutational analysis reveals that this glycosylation is dispensable for ligand binding and high expression in transfected cells. Metabolic labelling has revealed the receptor to also be sulphated and phosphorylated. Phosphorylation is ligand independent and is not enhanced by ligand binding and internalization, suggesting similarities with the viral chemokine receptor homologue US28. Like US28, an analysis of the full cellular complement of D6 in transfected cells indicates that $> 80\,\%$ is found associated with intracellular vesicular structures. This may account for the high quantities of D6 that can be synthesized in these cells. These unusual properties of D6, and the biochemical characterization described here, leads the way towards work aimed at generating the three-dimensional structure of this seven-transmembrane-spanning receptor.

Key words: chemokine, D6 chemokine receptor, G-protein, purification, structure.

INTRODUCTION

Chemokines are typically defined as regulators of the migration of cells, particularly leucocytes [1–8], but they also display a significant degree of pleiotropy, controlling processes as diverse as angiogenesis [9], proliferation [10,11] and apoptosis [12,13]. The chemokines are divided into four subfamilies, defined by variations on a conserved cysteine motif. The two largest subfamiles are defined by the presence of four cysteines in the mature protein. Chemokines in which the first two cysteines are separated by a single variable intervening amino acid are referred to as the CXC chemokines, while those in which the first two cysteines are juxtaposed are referred to as the CC chemokines. There are two smaller subfamilies, the XC and CX3C families, which are represented by only single members, namely lymphotactin and Fractalkine respectively.

The chemokines exert their actions through 7-TM (seven transmembrane spanning) GPCRs (G-protein-coupled receptors) [14]. There is a systematic nomenclature for these receptors: those for the CC-chemokines are called CCRs (of which 11 have been identified so far) and those for the CXC-chemokines are called CXCRs (currently six). There are single receptors for lymphotactin (XCR1) and Fractalkine (CX3CR1). In addition, two mammalian 7-TM receptor proteins, DARC (Duffy antigen receptor for chemokines) and D6, bind many pro-inflammatory chemokines, but do not appear to signal following this interaction [15,16]. These molecules are expressed on subsets of endothelial cells lining blood vessels (for DARC) or lymphatic channels (D6), and it is postulated that they may either transport chemokines across these microanatomical barriers or act as decoy receptors, internalizing and degrading chemokines ([16–19]; R. J. B. Nibbs, unpublished work).

Chemokine receptors are under intensive investigation as potential therapeutic targets [20], as they are central to the development of many human pathologies. For example, CCR5 and CXCR4 play clear and essential roles in mediating the cellular entry of HIV [21], and there is compelling evidence for the involvement of chemokine receptors in autoimmune and inflammatory disorders [22]. Furthermore, metastatic cancer cells may navigate using chemokine receptors [23], and some lymphomas are characterized by chemokine receptor expression and chemokine-directed tissue tropism [24].

Attempts to design chemokine receptor antagonists have been hampered by a lack of accurate structural models of chemokine receptors, with that of bovine rhodopsin being the only high-resolution 7-TM GPCR structure known [25,26]. One reason for this is the difficulty associated with expressing high levels of these receptors, including chemokine receptors, in heterologous transfectants. In contrast, mammalian cell lines can be generated that express extremely high levels (millions of receptors per cell) of D6 protein. Thus it is possible, in principle, to obtain enough D6 for crystallization. Here we describe the purification of milligram quantities of bioactive D6 receptor from transfected mammalian cells, characterize aspects of the biochemistry of the purified receptor and demonstrate that D6 is sulphated, decorated by N-linked glycosylation and phosphorylated in a ligand-independent

Abbreviations used: CHS, cholesteryl hemosuccinate; DARC, Duffy antigen receptor for chemokines; DDM, n-dodecyl β-D-maltoside; DTT, dithiothreitol; GFP, green fluorescent protein; GPCR, G-protein-coupled receptor; HA, haemagglutinin; HAD6H1, D6 with a C-terminal His_{10} tag and an N-terminal HA tag; MIP, macrophage inflammatory protein; 7-TM, seven-transmembrane-spanning.

[1] To whom correspondence should be addressed (e-mail g.graham@beatson.gla.ac.uk or neil@chem.gla.ac.uk).

manner. The present study is an essential prelude to the ultimate aim of generating high-resolution structural information from D6 crystals.

EXPERIMENTAL

Generation and expression of epitope-tagged D6 (HAD6H10)

Nucleotides encoding N-terminal HA (haemagglutinin) (MYPYDVPDYAG) and C-terminal His_{10} tags were introduced into human D6 cDNA by PCR, to generate HAD6H10. Products were verified by sequencing and cloned into pcDNA3.1 (Invitrogen, Paisley, U.K.). pcDNA3.1 or the HAD6H10 construct was transfected into L1.2 cells using Superfect (Qiagen, West Sussex, U.K.). Stable clones were selected in 1.6 mg/ml G418. Non-glycosylated epitope-tagged D6 was generated by mutating Asn^{17} in the putative NSS N-linked glycosylation site to QSS using the primers 5′-ATGCCGATTCTGAGCAGAGCAGCTTC-3′ and 5′-GAAGCTGCTCTGCTCAGAATCGGCAT-3′. Stable L1.2 clones expressing this mutant were generated as above.

Cell culture and flow cytometry

Tissue culture supplies were from Life Technologies (Paisley, U.K.) unless otherwise stated. Murine L1.2 pre-B cells were maintained in RPMI 1640 containing 5 mM glutamine, 10 % (v/v) heat-inactivated fetal calf serum (PAA Laboratories, Yeovil, Somerset, U.K.), 50 μM β-mercaptoethanol, and antibiotics. Small L1.2 cultures were grown in 5 % CO_2 at 37 °C. Large 10 litre cultures were grown in a 15 litre bioreactor (Applikon, Tewkesbury, U.K.) configured according to the manufacturer's instructions. HAD6H10 expression was enhanced by adding the histone deacetylase inhibitor sodium butyrate (Sigma, Poole, Dorset, U.K.) to 10 mM and culturing for 18 h prior to harvest. Flow cytometry was performed as described in [18].

Radioligand binding assays

We used a dimeric mutant of murine MIP-1α (macrophage inflammatory protein-1α) with wild-type bioactivity that binds with high affinity to D6 [16]. For ligand displacement assays, cells were harvested (5×10^5 cells/reaction in triplicate), washed with PBS, and resuspended in L1.2 culture medium (with 25 mM Hepes, pH 7.4, and 0.2 % sodium azide) containing 12 nM ^{125}I-MIP-1α and unlabelled MIP-1α up to 300 nM. To measure saturation binding, cells were incubated with increasing concentrations of ^{125}I-MIP-1α in the presence or absence of excess unlabelled competitor (each in triplicate). Reactions were incubated at room temperature for 90 min and then washed three times in PBS, and cell-associated radioactivity was read on a γ-counter.

Purification of HAD6H10

Clone 56 (10 litres) was harvested by centrifugation, washed twice in ice-cold PBS and resuspended in 50 ml of buffer A [20 mM phosphate buffer, 150 mM NaCl, 10 % (v/v) glycerol, pH 8.0]. At all stages, samples were kept on ice and Complete EDTA-free protease inhibitor cocktail tablets (Roche, Lewes, East Sussex, U.K.) were added as appropriate. Cells were disrupted using a French press ($\sim$6555 kPa; 950 lbf/in^2), and cell debris was removed by centrifugation (20 000 ***g***, 20 min). The supernatant was then centrifuged (120 000 ***g***; 1 h), and the membrane pellet was resuspended in 50 ml of buffer A containing 2 % (w/v) DDM (n-dodecyl β-D-maltoside; Glycon, Luckenwalde, Germany) and 0.05 % (w/v) CHS (cholesteryl hemisuccinate; Sigma) and stirred gently at 4 °C for 2 h. Insoluble material was removed by centrifugation (120 000 ***g***, 30 min). Solubilized membranes were applied to a 5 ml nickel Hitrap column (Amersham Biosciences) connected to an AKTA Purifier 100 (Amersham Biosciences), and a step gradient of imidazole in buffer B (buffer A containing 0.2 % DDM and 0.005 % CHS) was applied. HAD6H10 was eluted using 300 mM imidazole. Fractions identified as containing HAD6H10 by Western blotting were combined and the imidazole was reduced to 15 mM by dilution in buffer B. HAD6H10 was further purified and concentrated using 1 ml of Talon colbalt resin (BDClontech, Oxford, U.K.) and eluted with 150 mM imidazole. PD-10 columns (Amersham Biosciences) were used to remove the imidazole, and Centricon columns (Vivascience, Gottingen, Germany) were used for further concentration. Purified D6 was quantified using the BCA (bicinchoninic acid) assay (Pierce, Rockford, IL, U.S.A.).

SDS/PAGE and immunodetection of HAD6H10

Samples were run adjacent to MultiMark markers (Invitrogen) on 4–12 % (w/v) acrylamide gels according to the manufacturer's instructions (Invitrogen), with the exception that samples were routinely incubated in loading buffer [2 % (w/v) SDS, 25 mM DTT (dithiothreitol), 10 % (v/v) glycerol, 0.5 % Bromophenol Blue] at room temperature for 10 min prior to loading. Following electrophoresis, gels were either stained using Coomassie Blue or electrophoretically transferred to PVDF membrane for immunodetection. After overnight blocking in 10 % (w/v) dried milk/PBS, membranes were probed with anti-D6 monoclonal antibodies [18], anti-(horseradish peroxidase) antibodies (Roche) or anti-His-tag antibodies (Sigma). Anti-D6 and anti-His-tag blots were visualized with anti-(mouse horseradish peroxidase) secondary antibodies (Amersham Biosciences). Blots were developed via a chemiluminescence reaction (WestPico kit; Pierce). CCR5/D6 chimaeras have been used to show that anti-D6 antibodies recognize an epitope in the N-terminal domain of D6 (R. J. B. Nibbs, unpublished work).

Immunoprecipitation

Cells were washed with PBS, lysed with CellLytic buffer (Sigma), and the lysate was cleared by centrifugation (15 000 ***g***, 10 min). Portions of 1 ml of cleared lysate were incubated with anti-HA (Sigma) or anti-D6 [18] antibodies conjugated to Sepharose at 4 °C for 2 h. Sepharose beads were then washed twice with CellLytic buffer and four times with immunoprecipitation buffer [50 mM Tris, pH 7.5, 0.1 % (w/v) SDS, 150 mM NaCl]. Bound protein was released by the addition of 100 μl of HU buffer (8 M urea, 5 % SDS, 200 mM Tris/HCl, pH 8, 0.1 mM EDTA, 0.5 % Bromophenol Blue, 100 mM DTT) and visualized by immunoblotting.

Scintillation proximity assays

Purified HAD6H10 (100 ng) in 100 μl of PBS containing 20 % (v/v) fetal calf serum was added to the wells on a nickel-chelate FlashPlate (PerkinElmer, Cambridge, U.K.). Following incubation at room temperature for 1 h, the plates were washed with PBS/fetal calf serum prior to addition of ^{125}I-MIP-1β (Amersham Biosciences) to 40 pM. Unlabelled MIP-1α was also added up to 500 ng/ml. After 1 h in the dark at room temperature, the plates were washed three times with 100 μl of PBS/fetal calf serum, 100 μl of PBS was added, and the plates were read using a 1450 Microbeta Trilux (PerkinElmer).

Glycosylation analysis

The glycosylation of purified HAD6H10 was assessed using Pro-Q Fuchsia stain (Molecular Probes). Deglycosylation analysis was performed using a glycoprotein deglycosylation kit (Calbiochem, Nottingham, U.K.). Briefly, 5 μg portions of purified HAD6H10 were incubated with each glycosidase supplied, then the samples were separated by SDS/PAGE and immunoblotted using the anti-D6 antibody.

Metabolic labelling studies

Cells were starved in either phosphate-free RPMI (ICN Biomedical, Basingstoke, U.K.) or sulphate-free RPMI (JRH Biosciences, Andover, Hants., U.K.) for 1 h at 37 °C. Radiolabelled phosphate (25 mCi/ml) or sulphate (300 μCi/ml; Amersham Biosciences) was added, and the cells were incubated at 37 °C for 3 or 18 h respectively, washed in ice-cold PBS, lysed in 500 μl of CellLytic buffer (Sigma) and the lysate cleared (20 000 ***g***, 4 °C, 10 min). Aliquots of 200 μl of cleared lysate were incubated with 80 μl of Ni^{2+}-nitrilotriacetate resin (Qiagen) for 2 h at 4 °C. The resin was then washed three times in PBS, once in 50 mM Tris, pH 7.5, 0.1 % (w/v) SDS and 150 mM NaCl, and finally once more in PBS. Bound protein was eluted using 100 μl of HU buffer. Eluates were separated by SDS/PAGE, blotted on to PVDF membrane and exposed to film at − 70 °C.

Generation and use of a D6 ligand column

A non-aggregating, dimeric mutant of murine MIP-1α [16] was chemically synthesized with a C-terminal biotin tag by Albachem Ltd (Edinburgh, U.K.). A 20 μg aliquot of this protein was immobilized on streptavidin–agarose beads, and the MIP-1α-bearing beads were loaded on to a spin column using the ProFound kit (Pierce) according to the manufacturer's instructions. A D6-ligand-negative column was generated by following the above protocol but omitting the biotinylated MIP-1α. Then 100 ng of purified D6 in 100 μl of solution (0.05 % DDM, 0.0025 % CHS, 20 mM Tris, pH 7.5, and 150 mM NaCl) was applied to each column and incubated for 1 h at room temperature. Both columns were then washed three times with the supplied wash buffer (which had been brought to 0.05 % DDM and 0.0025 % CHS). Elution of bound D6 protein was performed in two steps. Initial elution was with 250 μl of the supplied elution buffer (again brought to 0.05 % DDM and 0.0025 % CHS) and a second elution was performed with 250 μl of HU buffer (see above). The presence of D6 in the various fractions obtained from these columns was evaluated by Western blotting using the anti-D6 monoclonal antibody as described above. The blots were quantitatively evaluated using a commercially available densitometry package provided by Total Lab Systems Ltd. (Auckland, New Zealand).

Subcellular visualization of D6–GFP (green fluorescent protein) fusion proteins

To produce a fusion cDNA capable of generating D6 with a C-terminal GFP tag, the full-length coding sequence for human D6, lacking the stop codon, was inserted into the pEGFPN2 vector (BDClontech, Oxford, U.K.). This plasmid was transiently transfected into either L1.2 cells or HEK293 cells using Superfect (Qiagen). A range of bioassays has shown the GFP-tagged receptor to be fully active in both of these cell backgrounds (results not shown). HEK293 cells were directly transfected in chambered slides. However, L1.2 cells were transfected in suspension and subsequently allowed to adhere to poly(L-lysine)-coated coverslips. Slides and coverslips were fixed with 4 % paraformaldehyde in PBS for 15 min at room temperature. The HEK293 cells were visualized directly on the slides following the addition of a coverslip, and the L1.2 cells were visualized following immobilization of the cell-bearing coverslips on microscope slides. GFP was detected by confocal microscopy using a Leica SP2 confocal.

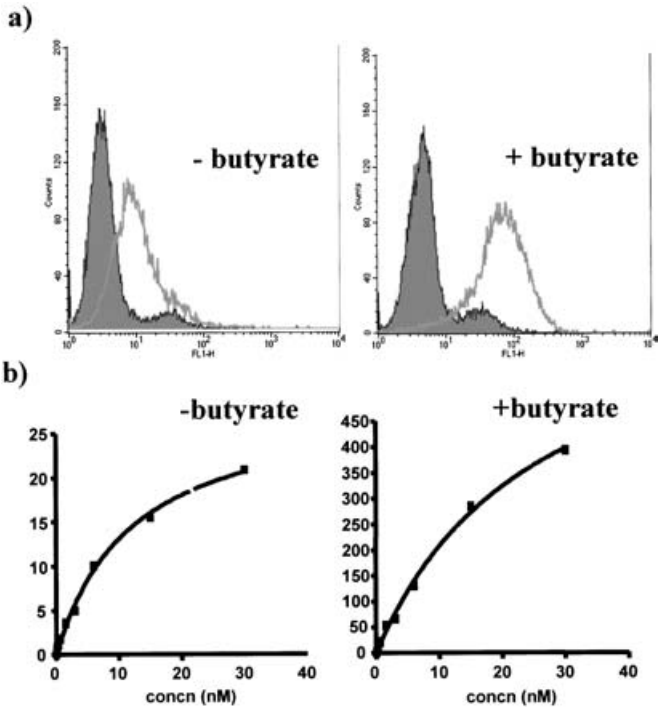

Figure 1 Expression of functional epitope-tagged D6 receptor on L1.2 cells

(**a**) Butyrate induction of D6 expression in transfected L1.2 cells. Vector control (filled) or HAD6H10-expressing (unfilled) L1.2 cells, treated with or without butyrate, were examined for D6 expression by flow cytometry using an anti-D6 antibody detected with a phycoerythrin-coupled anti-mouse IgG antibody. (**b**) Binding analysis of the epitope-tagged D6 receptor on L1.2 cells. Butyrate-treated and untreated HAD6H10-expressing cells were subjected to binding analysis using a range of concentrations of radiolabelled MIP-1α. Radioactivity (c.p.m.) associated with the cells after binding and washing is shown.

RESULTS

Generation and characterization of epitope-tagged D6

To facilitate the visualization and purification of the D6 protein, we have generated epitope-tagged D6 constructs encoding D6 with a C-terminal His_{10} tag and an N-terminal HA tag (HAD6H10). This construct was transfected into the L1.2 murine pre-B cell line and pools of transfectants obtained. Preliminary flow cytometric analysis of the level of cell surface D6 in these pools of transfected cells, using an anti-D6 monoclonal antibody [18], demonstrated only weak immunoreactivity, indicative of low surface expression of the receptor. However, overnight treatment with the histone deacetylase inhibitor sodium butyrate markedly enhanced D6 specific immunoreactivity, suggesting high levels of D6 expression to be achievable in butyrate-treated cells. An example of the butyrate-enhanced cell surface receptor levels in a clone of HAD6H10-transfected cells is shown in Figure 1(a). As can be seen, there was a 10-fold increase in cell surface D6 in these cells following butyrate treatment. Curiously, butyrate treatment is not required to achieve high-level expression of D6 in other cell types, suggesting that some aspect of L1.2 cell biology

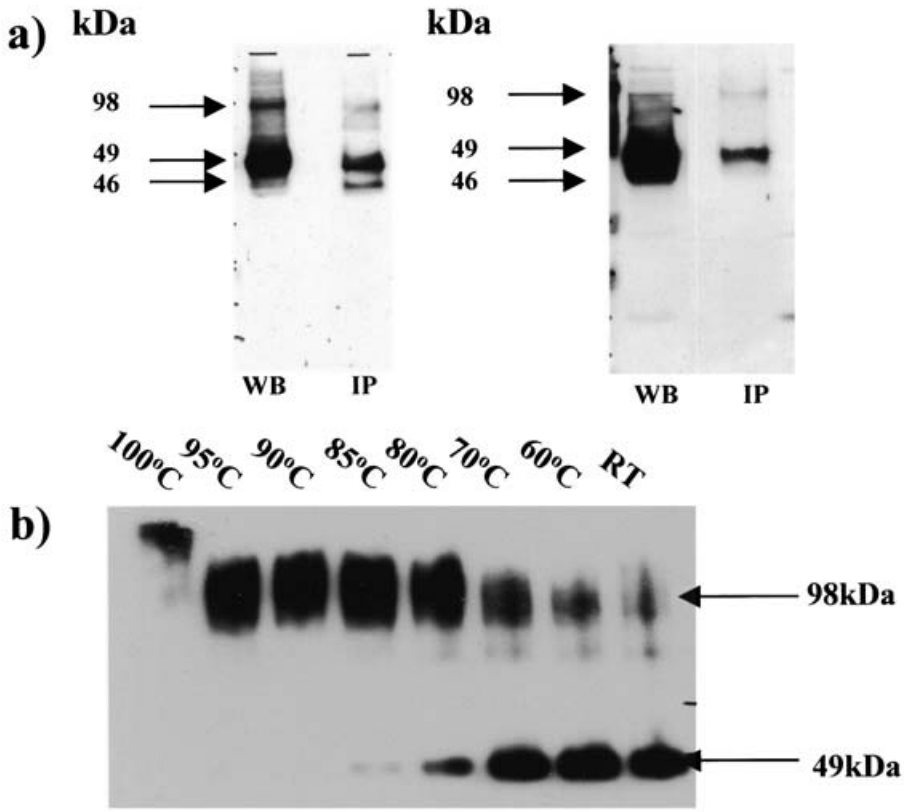

Figure 2 D6 protein analysis

(**a**) Western blot assessment of D6 protein. Butyrate-treated L1.2 cells expressing epitope-tagged D6 were lysed, and D6 in the lysates (lanes WB) or in immunoprecipitates from the lysates (lanes IP) was visualized on Western blots probed with anti-HA (left panel) or anti-D6 (right panel) antibodies. (**b**) Impact of temperature on the resolution of D6 protein by SDS/PAGE. Membranes from L1.2 cells expressing epitope-tagged D6 proteins were lysed in SDS/DTT and treated at the indicated temperatures prior to running on SDS/PAGE gels and immunodetection using anti-HA antibody. The positions of the D6 dimer and monomer are indicated.

is responsible for the relative silencing of the vector-expressed D6 in this cell line in the absence of inducing agents.

Using radioligand binding assays, a number of transfected clones expressing high surface levels of HAD6H10 were isolated and one of these, clone 56, was selected for further study. Scatchard analysis of saturation radioligand binding data (Figure 1b) showed that there were $\sim 35\,000$ receptors per cell, with a K_D of 12 nM. However, following butyrate treatment, the cells had approx. 880 000 surface receptors per cell, with a slightly increased K_D of 25 nM. These data therefore demonstrate that the epitope-tagged D6 protein binds D6 ligands with high affinity, confirming retention of function in the epitope-tagged receptor.

Initial Western blot analysis of the tagged D6 protein, using anti-HA antibodies, was confounded by difficulties in separating and visualizing the HAD6H10 protein on SDS/PAGE gels. Optimal conditions for D6 analysis by SDS/PAGE were determined empirically (see below) and involved SDS/DTT treatment of the membrane preparations at room temperature for 10 min. Using this methodology, and using an anti-HA antibody to visualize the protein on Western blots, HAD6H10 was seen to be present predominantly as a monomeric species with a molecular mass of approx. 49 kDa (Figure 2a). The expected molecular mass of the epitope-tagged receptor is 46.1 kDa, suggesting post-translational decoration of the protein (see below). Frequently a slightly smaller band of 46 kDa was also seen, and the identity of this band is discussed in more detail below. In addition, evidence of HAD6H10 aggregation was obtained from the Western blots, and the presence of an anti-HA reactive species with an apparent molecular mass of 98 kDa was also seen, indicative of the presence of an SDS-stable D6 dimer in the membrane preparations. Upon prolonged exposure, higher-molecular-mass species were also evident, indicating further SDS-stable aggregation to be a feature of the tagged D6 receptor. Proteins with similar molecular masses were also seen in Western blots probed with an anti-D6 antibody, and indeed immunoprecipitation by anti-HA or anti-D6 antibodies pulled down similar protein species (Figure 2a).

To examine the apparent dimerization further, we analysed the impact of heating during protein preparation on the extent of HAD6H10 aggregation. Previous analyses indicated that boiling membrane preparations in the presence of SDS/DTT induced extensive aggregation of the D6 protein, which prevented it from entering the gel. A survey of the effects of reducing the treatment temperature (Figure 2b) indicated that the presence of the dimeric, or higher-order, species is highly temperature dependent. Indeed, above 80 °C the protein visualized by SDS/PAGE was predominantly aggregated (dimeric and larger), whereas at lower temperatures it was largely monomeric. Therefore it appears that dimeric and higher-order aggregated species may be related more to the method of protein preparation for SDS/PAGE rather than to receptor function.

Thus, as visualized by SDS/PAGE, HAD6H10 was predominantly monomeric, with an apparent molecular mass of 49 kDa. Evidence of higher-order structures was also seen both on Western blots and by immunoprecipitation, although the extent of aggregation of the D6 protein observed in SDS gels appeared to be unaffected by ligand (results not shown). Together, these

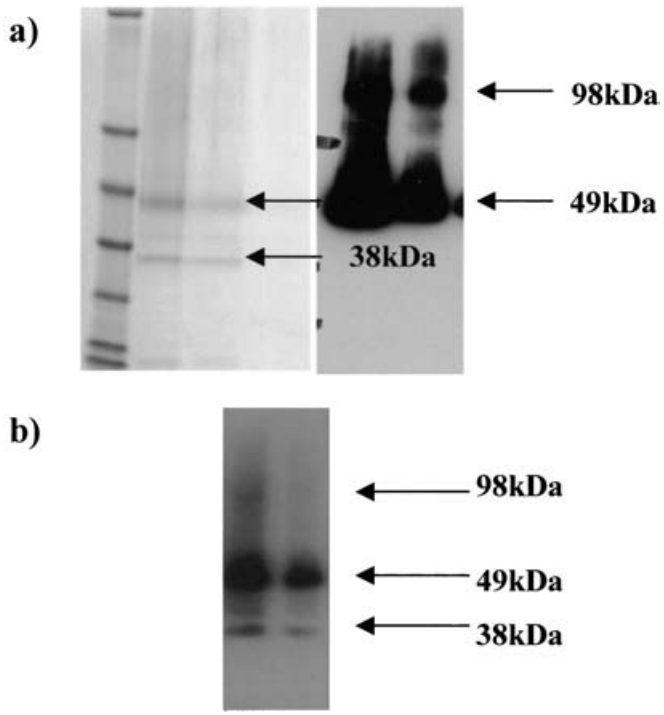

Figure 3 Analysis of purified tagged D6

(**a**) SDS/PAGE and Western blot analysis of purified D6 protein. D6 protein was visualized using Coomassie Blue staining (left panel) or Western blotting using an anti-HA antibody (right panel). (**b**) Western blot detection of purified D6 protein using anti-His-tag antibody. Note the presence of the 38 kDa protein on the blots.

data suggest that the higher-order species seen on SDS/PAGE gels either may represent a low level of ligand-independent receptor dimerization in cells, or alternatively could reflect a tendency for D6 to aggregate during sample preparation.

Purification of D6

HAD6H10 was purified from bulk cultures of transfected L1.2 cells as described in the Experimental section. Following elution from the cobalt affinity gels, and in keeping with the previous Western blot data (Figure 2a), SDS/PAGE analysis and Coomassie Blue staining of the purified D6 protein revealed a predominant band of approx. 49 kDa, with a lower-molecular-mass band of 38 kDa also being evident (Figure 3a). Blotting of these gels and probing with an anti-HA antibody revealed the 49 kDa band to be cross-reactive, indicating the presence of the HA tag. In addition, higher-order protein structures, including the 98 kDa band observed in the initial SDS/PAGE analysis of membranous D6 protein, were also apparent. Thus this Western blot analysis confirms the purified protein to be D6. The 49 kDa and higher-molecular-mass proteins were also detected by anti-D6 antibodies (results not shown), and in addition were detected by antibodies to the C-terminal His tag (Figure 3b). Intriguingly, the 38 kDa band did not cross-react with either the anti-D6 or anti-HA antibodies, although it did cross-react with the anti-His-tag antibody, suggesting that it may be an N-terminal cleavage product of full-length D6.

Despite numerous attempts, the 49 kDa band did not generate any identifiable peptide fragments following trypsinization and analysis by electrospray MS. The 38 kDa band did, however, yield three tryptic peptides identified as being derived from D6 (Table 1). These included a peptide derived from the N-terminal

Table 1 Tryptic fragments of D6 detected by MS

Peptide	Sequence	Position in D6
1	KDAVVSFGK	Immediately N-terminal to the first transmembrane region
2	MVSTLYTINFYSGIFFISCMSLDK	Third transmembrane region
3	QSENYPNKEDVGNK	Extreme C-terminus

extracellular domain of D6, a peptide spanning the bulk of the third transmembrane domain and a peptide derived from the extreme C-terminus of the protein. The fact that the MS data indicated that the 38 kDa band was clearly derived from D6, plus the observation that it was detected by the anti-His tag antibody but not by either of the N-terminal antibodies, again suggests that this is an N-terminal cleavage derivative of full-length D6. Interestingly, neither the full-length nor the apparently N-terminally cleaved D6 proteins were amenable to N-terminal sequencing, suggesting that both are N-terminally blocked, although the mechanism whereby the putative cleaved receptor is N-terminally blocked is not at present apparent.

Sufficient purified D6 protein was generated to enable analysis of secondary structure using CD. This analysis revealed the purified protein to be substantially α-helical, in keeping with the expected 7-TM structure. Furthermore, these data suggested maintenance of secondary structure in the purified protein (results not shown).

Thus DDM solubilization and metal chelate chromatography resulted in the purification of a tagged D6 protein which was substantially α-helical, but which was not, in its intact form, amenable to N-terminal sequencing or MS analysis.

Receptor binding assays do not predict total levels of D6 protein

The production of large amounts of purified D6 protein has allowed us to examine the ability of receptor binding assays to predict actual levels of D6 protein in expressing cells. To this end, we have estimated receptor numbers in ligand binding assays and have then determined the amount of receptor protein in the membrane preparations by Western blot, comparing the Western blot signals with those obtained using known amounts of purified, tagged D6 protein. As shown in Figure 4(a), whereas receptor binding assays predicted between 200000 and 600000 receptors per butyrate-treated cell, there was little, if any, relationship between these receptor numbers and the actual amount of protein detected using anti-D6 antibodies on Western blot. More accurate Western blot-based quantification of amounts of receptor protein per cell suggested that butyrate-treated cells were expressing up to 1 mg of tagged D6 protein per 5×10^9 cells. This is equivalent to approx. 2.5×10^6 receptor molecules per cell, further suggesting that the ligand displacement assays grossly underestimate receptor numbers. Thus Western blot analysis indicates that, at any one time, only 10–20 % of total cellular D6 receptor is on the cell surface, with the rest presumably being present in intracellular stores.

To investigate the nature of these intracellular stores, we generated a C-terminally GFP-tagged variant of D6 which retains full biological activity in ligand binding assays (results not shown; M. Weber, E. Blair, M. O'Hara, C. V. Simpson, P. E. Blackburn, A. Rot, G. J. Graham and R. J. B. Nibbs, unpublished work). Initial studies using transfected L1.2 cells revealed the majority of the D6–GFP protein to be present in intracellular vesicles, with little cell surface fluorescence being evident (Figure 4b). These cells have a very high nuclear/cytoplasmic ratio, and thus clear visualization of the cytoplasmic localization of the transfected

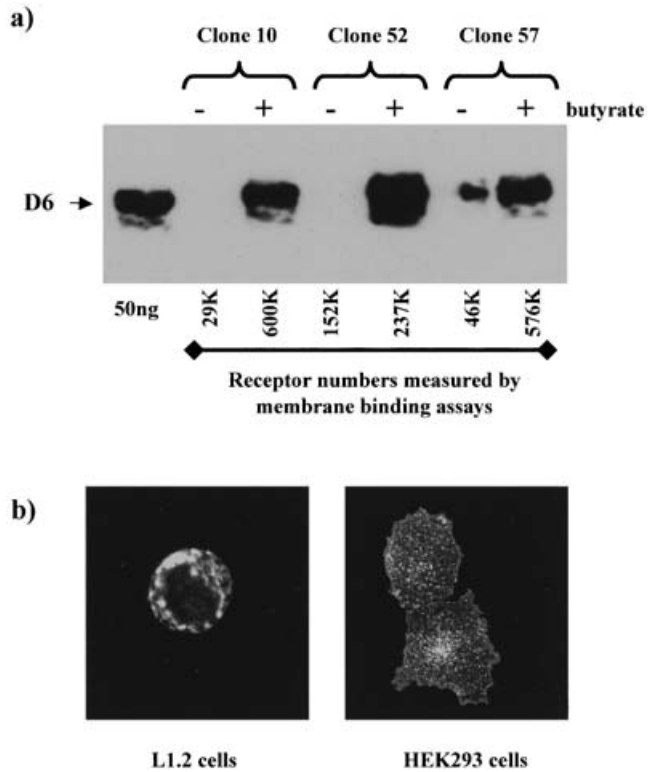

Figure 4 The bulk of D6 protein is found intracellularly

(**a**) Western blotting reveals discordance between binding data and actual receptor protein levels. Surface receptor levels in three clones of untreated or butyrate-treated D6-expressing L1.2 cells, as assessed using standard ligand binding assays, are shown at the bottom of the Figure. In parallel, equal numbers of cells from each cell line (+/− butyrate) were lysed and the amounts of D6 protein assessed using Western blotting in comparison with a known amount of purified D6 protein. D6 was revealed using the anti-D6 antibody. (**b**) D6 is associated predominantly with intracellular vesicles. The intracellular distribution of D6 was investigated by transfecting vectors incorporating a D6–GFP fusion cDNA into L1.2 cells (left panel) and HEK293 cells (right panel). The cells were visualized by confocal microscsopy.

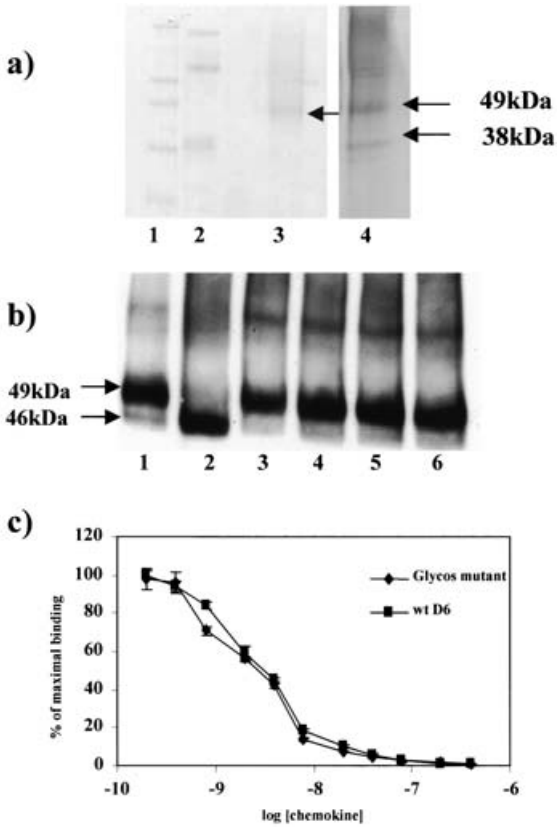

Figure 5 D6 is glycosylated, but this is not required for ligand binding

(**a**) Fuchsia staining detects the presence of glycosylation in purified D6 protein. Lanes 1 and 2, molecular mass and glycosylation standards, lane 3, purified D6 protein; lane 4, Coomassie Blue staining of the purified D6 protein to confirm protein sizes. The positions and sizes of the protein bands are indicated by the arrows. (**b**) Glycosidase treatment reveals D6 to be N-glycosylated. Lane 1, no enzymic treatment; lane 2, N-Glycosidase F; lane 3, endo-α-*N*-acetylgalactosaminidase, lane 4, α-2–3,6,8–9-neuraminidase; lane 5, β1–4-galactosidase; lane 6, β-*N*-acetylglucosaminidase. Digested preparations were visualized by Western blotting with anti-D6 monoclonal antibody. The positions of the 49 and 46 kDa bands are indicated by the arrows. (**c**) A deglycosylated mutant version of D6 binds chemokine. Displacement of ^{125}I-MIP-1α by unlabelled MIP-1α was used to examine the affinity of MIP-1α for wild-type (wt) and non-glycosylated D6 expressed in L1.2 cells.

GFP-tagged D6 protein is difficult. To enhance our ability to visualize the subcellular distribution of D6–GFP, we also examined its localization in transfected HEK293 cells, which have a more expansive cytoplasmic compartment. Again, in these cells, the majority of D6 was seen in discrete, albeit smaller, intracellular vesicles, with only a minority being present on the cell membrane (Figure 4b). Further work by us has demonstrated these vesicles to be within the recycling endosomal compartment (M. Weber, E. Blair, M. O'Hara, C. V. Simpson, P. E. Blackburn, A. Rot, G. J. Graham and R. J. B. Nibbs, unpublished work). These data therefore reveal a discordance between amounts of D6 receptor as measured by receptor binding assays and those measured by Western blot, with the majority of the D6 protein being present in intracellular, cytoplasmic vesicles. The relevance of these observations to the analysis of other receptors is not yet clear; however, they do suggest that caution should be exercised over the interpretation of cell surface binding data.

D6 is N-glycosylated, but this is not required for ligand binding

Production of purified HAD6H10 protein has allowed us to directly examine the glycosylation status of the receptor. Initial staining of SDS/PAGE gels of purified D6 with glycosylation-specific stains revealed the tagged D6 protein to be glycosylated (Figure 5a). Interestingly, and in keeping with the conclusion that the HAD6H10-derived 38 kDa band is an N-terminal cleavage product of the full-length protein (Figure 3a), this band was not stained with the glyco stain, suggesting the cleavage to be C-terminal to the putative glycosylation site. The purified D6 protein was then digested by a range of glycosidases and the effects on molecular mass assessed by Western blot (Figure 5b). As shown, HAD6H10 is amenable to digestion by N-glycosidase F (lane 2), indicating the presence of N-linked glycosylation on the tagged D6 protein. This is in keeping with the presence of an N-linked glycosylation site at the N-terminus of D6. As detailed above (Figure 2a), Western blot revealed two bands at approx. 49/46 kDa, but curiously only the upper band was detectable by the glycosylation-specific Fuchsia stain. Furthermore, upon digestion with N-glycosidase F, all D6 immunoreactive protein co-migrated with the lower band. This suggests that the lower band is non-glycosylated D6 which has presumably been purified from intracellular membranes before being glycosylated. No evidence for O-linked gycosylation was seen in the digests (Figure 5b, lanes 3–6).

As mentioned above, while the 38 kDa protein in the purified preparations (Figure 3a) was identifiable as being derived from D6 by tryptic MS, this methodology was unable to confirm

the D6 identity of the upper, and apparently full-length, 49 kDa band. Previous reports indicating potential difficulties involved in analysing glycosylated proteins by MS [27] suggested that the D6 glycosylation may be hampering analysis of the full-length protein by MS. Therefore we repeated the MS analysis using an enzymically deglycosylated 49 kDa band. Intriguingly, and in contrast with the glycosylated protein, deglycosylated D6 did yield a tryptic peptide (peptide 1 in Table 1) which was identified as being derived from D6. Thus N-linked glycosylation on D6 interfered with MS analysis, and only upon deglycosylation was full-length D6 identifiable by MS.

The presence of N-linked glycosylation and possible associated microheterogeneity, as well as the presence of a subspecies of non-glycosylated protein, may complicate attempts at crystallizing D6. Therefore, in an attempt to alleviate this potential problem and to examine the importance of N-linked glycosylation for D6 function, we generated a mutant version of epitope-tagged D6 in which we mutated the single D6 N-linked glycosylation site. Consistent with its deglycosylated status, this mutant receptor displayed an apparent molecular mass of 46 kDa on SDS/PAGE gels (results not shown). Radioligand binding analysis of this mutant non-glycosylated receptor (Figure 5c) indicated that it is able to bind murine MIP-1α; in addition, in homologous displacement assays, MIP-1α displayed a half-maximal displacement of radiolabelled tracer at a concentration that was indistinguishable from that seen with the wild-type receptor. Thus these data indicate that while D6 is N-glycosylated, it does not appear to require this glycosylation for ligand binding, and suggest that this deglycosylated variant may be a better candidate for crystallization than the wild-type protein.

D6 is sulphated in a glycosylation-independent manner

We also examined the sulphation status of the purified, tagged D6 receptor. N-terminal sulphation of chemokine receptors has been reported previously [28,29] and is believed to be important for ligand interactions. To circumvent the possible complication that sulphate labelling could occur on tyrosine residues or carbohydrate units, we assessed sulphation using both the epitope-tagged wild-type receptor and the non-glycosylated mutant mentioned above.

Metabolic labelling of D6-expressing and control cells followed by purification of the D6 protein and SDS/PAGE revealed (Figure 6a) clear sulphation of the wild-type D6 receptor (lane 1). This was maintained in the non-glycosylated mutant (lane 3), which migrated with an apparent molecular mass of 46 kDa, as predicted by the results of the deglycosylation studies. No sulphation of similar proteins was seen in the control L1.2 cells (lane 2). Thus these data demonstrate that D6 is sulphated in a glycosylation-independent manner.

D6 is phosphorylated in a ligand-independent manner

Previously, we have reported an apparent inability of D6 to signal following ligand binding [16]. More recently, a role for D6 as a non-signalling decoy receptor has been proposed [19]. Having determined the conditions under which epitope-tagged D6 can be purified, we set about examining the phosphorylation status of D6 and the impact of ligand binding on the level of phosphorylation. As shown in Figure 6(b), D6 was clearly phosphorylated in the absence of ligand, with prominent phosphoprotein bands of 49 and 98 kDa being evident (lane 1). Intriguingly, the addition of ligand had no apparent effect on D6 phosphorylation (lane 2), indicating that D6 is constitutively phosphorylated in a ligand-independent manner. Very few phosphoproteins were seen in the control cells (lane 3), suggesting that many of the additional bands

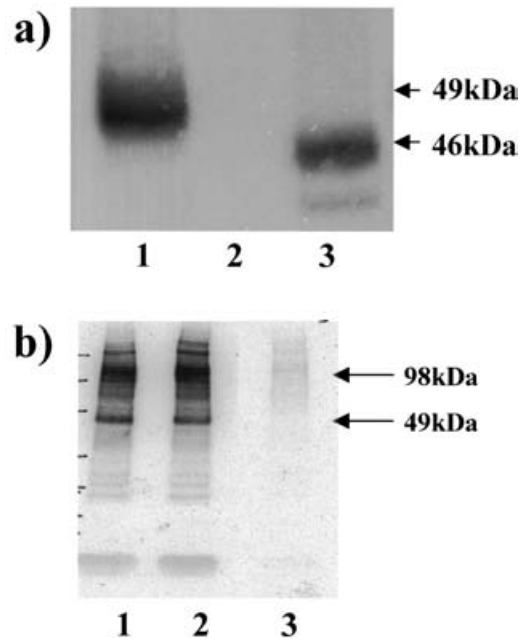

Figure 6 D6 is phosphorylated and sulphated

(**a**) D6 is sulphated in a glycosylation-independent manner. Cells labelled with radiolabelled sulphate were lysed and processed for D6 purification. Protein preparations were analysed by SDS/PAGE. Lane 1, L1.2 cells expressing glycosylated D6; lane 2, L1.2 cells expressing vector alone; lane 3, L1.2 cells expressing the non-glycosylated mutant of D6. (**b**) D6 is phosphorylated in a ligand-independent manner. D6 isolated from radiolabelled phosphate-loaded cells was run on SDS/PAGE gels, blotted and exposed to X-ray film. Lane 1, D6-expressing L1.2 cells plus ligand; lane 2, D6-expressing L1.2 cells with no ligand; lane 3, control L1.2 cells with ligand. Monomeric and dimeric D6 protein bands in the D6 transfectants are indicated. Equal loading was confirmed by Western blotting.

in lanes 1 and 2 were either aggregates of D6 or D6-associated proteins. In addition, and in agreement with results outlined above (Figure 2), the phosphoprotein analysis showed that there was no enhancement of levels of SDS-stable dimers or higher-order aggregates of D6 following ligand binding. This again suggests that ligand binding does not alter the relative proportions of aggregated compared with monomeric forms of D6, as visualized by SDS/PAGE.

Purified D6 protein is bioactive

Clearly, while solubilization by detergents such as DDM aids in the purification of the receptor, this may also compromise receptor function. Therefore, to test whether the purified, DDM-solubilized receptor was bioactive, we examined the ability of the purified receptor to bind ligand. This involved the use of FlashPlates on to which the purified epitope-tagged D6 protein was immobilized through its C-terminal His tag. Function was tested by directly examining the competable binding of a radiolabelled chemokine to the immobilized receptor. In this experiment, we used a constant amount of the radiolabelled D6 ligand MIP-1β (40 pM) and examined the ability of increasing amounts of unlabelled MIP-1α to displace the MIP-1β from the D6 receptor. As shown in Figure 7(a), we have been able to demonstrate competable binding of radiolabelled MIP-1β to the immobilized purified HAD6H10 protein. Unlabelled MIP-1α competed very effectively with the radiolabelled tracer MIP-1β for binding to the immobilized D6, displaying an EC_{50} of 88 pM.

One disadvantage of these assays is that they do not allow us to assess the fraction of the purified D6 receptor that is functional,

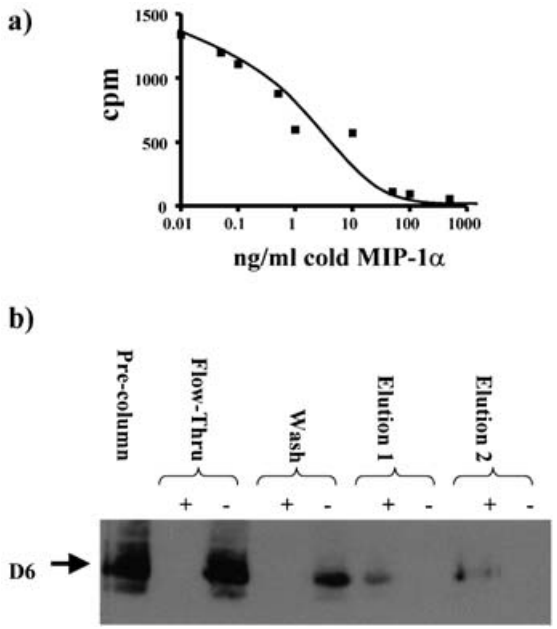

Figure 7 Purified D6 is bioactive

(**a**) Purified D6 binds ligand in a competable manner. The ability of purified D6 to bind ligand was assessed using FlashPlate binding assays. Portions of 100 ng of purified D6 were applied to wells in a 96-well FlashPlate and incubated with ^{125}I-MIP-1β (40 pM), which was displaced using various concentrations of unlabelled ('cold') MIP-1α. (**b**) Purified D6 binds completely to a MIP-1α affinity column. The fraction of active D6 within the purified preparations was assessed by applying D6 to a MIP-1α-bearing column. This Figure shown is a Western blot indicating the concentrations of D6 loaded on to the column (Pre-column), in the non-binding fraction (Flow-Thru) and eluted following washing or elution. Note that the bound receptor was eluted in a volume that was five times the volume loaded, and thus recovery was much higher than is apparent from this blot. For each wash or elution step, − refers to the control column and + refers to the MIP-1α-bearing column.

but simply indicate the presence of functional receptors within the pool of purified molecules. Therefore, to determine more accurately the fraction of the purified D6 protein that is active in terms of ligand binding, we produced a D6–ligand affinity column by immobilizing biotinylated MIP-1α to streptavidin–agarose beads. Purified D6 was applied to these columns on the assumption that only the active, correctly folded, receptor would bind, whereas the incorrectly folded, or inactive, receptor would simply flow through the column. This was evaluated using Western blotting. As shown in Figure 7(b), whereas the purified D6 protein displayed no binding to a control column which had no bound MIP-1α, it bound completely to the MIP-1α-bearing column (− and + Flow-Thru lanes respectively). Wash buffer removed residual D6 from the control column, but did not wash any D6 from the MIP-1α column. Elution using two separate elution buffers resulted in the successful removal of bound D6 protein from the MIP-1α column, but did not remove any D6 protein from the control column. Note that whereas the intensities of the bands obtained from the two elutions appear to be lower than in the pre-column fraction, densitometric analysis taking into account the dilutions occurring during the elution phases indicated essentially complete recovery of the D6 protein from the MIP-1α-bearing column. Thus these data indicate that the purified D6 protein binds to MIP-1α-bearing agarose beads, but does not bind to non-MIP-1α-bearing beads. The completeness of the binding of D6 to the MIP-1α beads and the ability to recover essentially all of the bound D6 protein (as assessed by densitometry) suggests that the majority, if not all, of the purified D6 is bioactive. These data therefore indicate that the purified receptor is fully bioactive and binds ligand with a high affinity.

DISCUSSION

A major issue slowing progress towards the ultimate determination of the full three-dimensional structure of GPCRs is the difficulty in producing large quantities of these proteins in a functional form. The use of bacterial, yeast or insect expression systems to enhance GPCR production has, in some instances, been of great value, but the purified receptors often have compromised activity [31–35]. Codon optimization strategies have been used to enhance production of the chemokine receptors CCR5 [36] and CXCR4 [37]. These purified receptors retain functional activity and can be incorporated into paramagnetic liposomes, in which they bind ligand as well as appropriate HIV gp120 proteins [30,37]. However, we have capitalized on the exceptionally high expression of D6 in transfected mammalian cells to produce approx. 0.5 mg of D6 protein per litre of cells. This protein can be purified and retains full biological activity.

The purified tagged D6 receptor is predominantly monomeric on SDS/PAGE, showing an apparent molecular mass of ~49 kDa, with a ~46 kDa species representing a non-glycosylated form. Higher-molecular-mass forms appear to represent SDS-stable dimers and higher-order structures. Such SDS-stable aggregation of GPCRs has been reported previously [38], and sensitivity to heating and other treatments shown. The difficulty in resolving D6 following heat pretreatment is similar to that seen with other membrane proteins, suggesting that care must be taken in pre-gel treatments of significantly hydrophobic proteins if proper resolution of the protein species is to be achieved [39]. There is much discussion in the literature about the potential relevance of chemokine receptor oligomerization for function [40]. With D6, this oligomerization is observed regardless of the presence or absence of ligand, and either results from the method of preparation or represents steady-state ligand-independent aggregation of the receptor, stabilized by SDS.

We have also identified a smaller peptide of ~38 kDa which is detected by an anti-His tag antibody and yields D6 peptide fragments following tryptic MS. It is not detected by anti-D6 or anti-HA antibodies, and is not glycosylated, suggesting that it is an N-terminal cleavage product. This species is not always apparent in the purified receptor preparations, and we hypothesize that there exists a 'fragile site' in the N-terminal domain of D6 responsible for the generation of this cleaved form. Sub-monomeric receptor species are also seen in other purified chemokine receptor preparations [36,37], and thus the presence of a breakage-susceptible N-terminal motif may be a more general feature of chemokine receptors.

D6 can be N-glycosylated on the predicted N-linked glycosylation site in the N-terminus. Interestingly, glycosylation interfered with MS-based formal identification of the full-length D6 protein. Only upon deglycosylation was the full-length receptor identifiable by tryptic MS, as has been reported previously for other proteins [27]. As a non-N-glycosyated mutant of D6 could be expressed to high levels and was fully functional in ligand binding, the role for this decoration remains to be determined. However, the availability of bioactive non-glycosylated D6 may enhance our chances of successful crystallization by minimizing the microheterogeneity that might otherwise be present in preparations of the purified wild-type receptor. In addition to glycosylation, we have obtained evidence of sulphation (presumably tyrosine linked) of D6. Sulphation of chemokine receptors has been reported [28,29] and is believed to be important for ligand

binding and HIV entry through the co-receptors CCR5 and CXCR4. In D6, which is not a significant receptor for HIV isolates, it remains to be shown whether sulphation is important for ligand binding.

Typically, phosphorylation is enhanced in chemokine receptors following ligand binding [41,42] and is important for GPCR internalization. D6 is constitutively phosphorylated, a modification apparently unchanged by ligand binding, reinforcing the atypical nature of this receptor. Results from our laboratories suggest that D6 is constitutively internalizing and recycling in expressing cells in the absence of chemokine (M. Weber, E. Blair, M. O'Hara, C. V. Simpson, P. E. Blackburn, A. Rot, G. J. Graham and R. J. B. Nibbs, unpublished work). Interestingly, US28, a cytomegalovirus-encoded chemokine receptor which displays a similar level of ligand promiscuity to D6, is also constitutively phosphorylated and exhibits ligand-independent signalling and internalization [43,44]. This has been implicated in its ability to remove chemokines from the milieu of expressing cells, and D6 may use a similar mechanism in its proposed role as a decoy receptor. Another feature common to both D6 and US28 is that the surface levels of these receptors represent only a fraction of the total cellular receptor pool [44]. With D6, only 10–20 % is on the cell surface at any one time, and similar results have been seen with US28. Studies presented here (Figure 4b) and further studies by us (M. Weber, E. Blair, M. O'Hara, C. V. Simpson, P. E. Blackburn, A. Rot, G. J. Graham and R. J. B. Nibbs, unpublished work) have revealed that, following GFP tagging, D6 can be detected by confocal microscopy in discrete intracellular vesicles in transfected cells. Little cell surface receptor staining is seen in these transfectants, and this contrasts sharply with other chemokine receptors such as CCR5, which are seen prominently associated with the plasma membrane ([45]; M. Weber, E. Blair, M. O'Hara, C. V. Simpson, P. E. Blackburn, A. Rot, G. J. Graham and R. J. B. Nibbs, unpublished work). We believe that these vesicles contain the bulk of intracellular D6 and form a recycling pool of receptors which are likely to be rapidly mobilizable. The ability to rapidly mobilize such pools of decoy receptors may be important under conditions of inflammatory stress. It remains formally possible that, while we have demonstrated glycosylation as well as constitutive sulphation and phosphorylation within our population of purified D6 molecules, the intracellular and cell surface pools of receptors may display differential levels of post-translational modification which may have an impact on receptor funtion. We have attempted to examine the relative levels of phosphorylation, sulphation and glycosylation of the intracellular and cell surface D6 molecules by specifically precipitating cell surface receptors following biotinylation of total membrane proteins in L1.2 cells. While the residual pool of cytoplasmic D6 molecules is rich enough to allow easy visualization of the protein, even when using large numbers of cells we were unable to obtain enough cell surface D6 to allow assessment of the level of post-translational processing. Nevertheless, the biological assays outlined in Figure 7 suggest that even if there is differential post-translational processing of cell surface and intracellular receptors, this is unlikely to have implications for function, as all of the purified receptor molecules appear to be active in binding ligand.

In conclusion, the present study describes the purification and characterization of functional D6. To our knowledge, the heterologous expression and purification of such high quantities of bioactive chemokine receptor are unprecedented. This represents an important prelude to the eventual determination of the structure of this receptor.

We thank Dr A. Pitt, Professor N. Price and Dr S. Kelly for help with MS and CD, and Dr A. Alcami and Dr G. Douce for advice and assistance with the FlashPlate assays. This study was supported by a grant from the Biotechnology and Biological Sciences Research Council (N. W. I., G. J. G., R. J. B. N.). Work in the laboratories of G. J. G. and R. J. B. N. is funded by grants from Cancer Research U.K.

REFERENCES

1 Rollins, B. J. (1997) Chemokines. Blood **90**, 909–929
2 Zlotnik, A. and Yoshie, O. (2000) Chemokines: A new classification system and their role in immunity. Immunity **12**, 121–129
3 Mantovani, A. (1999) The chemokine system: redundancy for robust options. Immunol. Today **20**, 254–259
4 Melchers, F., Rolink, A. G. and Schaniel, C. (1999) The role of chemokines in regulating cell migration during humoral immune responses. Cell **99**, 351–359
5 Rossi, D. and Zlotnik, A. (2000) The biology of chemokines and their receptors. Annu. Rev. Immunol. **18**, 217–229
6 Doitsidou, M., Reichman-Fried, M., Stebler, J., Koprunner, M., Dorries, J., Meyer, D., Esguerra, C. V., Leung, T. and Raz, E. (2002) Guidance of primordial germ cell migration by the chemokine SDF-1. Cell **111**, 647–655
7 Knaut, H., Werz, C., Geisler, R. and Nusslein-Volhard, C. (2003) A zebrafish homologue of the chemokine receptor CXCR4 is a germ cell guidance receptor. Nature (London) **421**, 279–285
8 Tsai, H. H., Frost, E., To, V., Robinson, S., ffrench-Constant, C., Geertman, R., Ransohoff, R. M. and Miller, R. H. (2002) The chemokine receptor CXCR2 controls positioning of oligodendrocyte precursors in developing spinal cord by arresting their migration. Cell **110**, 373–381
9 Strieter, R. M., DiGiovine, B., Polverini, P. J., Kunkel, S. L., Shanafelt, A., Hesselgesser, J., Horuk, R. and Arenberg, D. A. (1999) CXC chemokines and lung cancer angiogenesis. In Chemokines and Cancer (Rollins, B. J., ed.), pp. 143–157, Humana Press, Clifton, NJ
10 Graham, G. J. (1997) Growth inhibitors in haemopoiesis and leukaemogenesis. Balliere's Clin. Haematol. **10**, 539–547
11 Cashman, J., Clark-Lewis, I., Eaves, A. and Eaves, C. (2002) Stromal-derived factor 1 inhibits the cycling of very primitive human hematopoietic cells *in vitro* and in NOD/SCID mice. Blood **99**, 792–799
12 Bakhiet, M., Tjernlund, A., Mousa, A., Gad, A., Stromblad, S., Kuziel, W. A., Seiger, A. and Andersson, J. (2001) RANTES promotes growth and survival of human first-trimester forebrain astrocytes. Nat. Cell Biol. **3**, 150–155
13 Lataillade, J. J., Clay, D., Bourin, P., Herodin, F., Dupuy, C., Jasmin, C. and Le Bousse-Kerdiles, M. C. (2002) Stromal cell-derived factor 1 regulates primitive hematopoiesis by suppressing apoptosis and by promoting G(0)/G(1) transition in CD34(+) cells: evidence for an autocrine/paracrine mechanism. Blood **99**, 1117–1127
14 Murphy, P. M., Baggiolini, M., Charo, I. F., Herbert, C. A., Horuk, R., Matsushima, K., Miller, L. H., Oppenheim, J. J. and Power, C. A. (2000) International Union of Pharmacology. XXII. Nomenclature for chemokine receptors. Pharmacol. Rev. **52**, 145–156
15 Szabo, M. C., Soo, K. S., Zlotnik, A. and Schall, T. J. (1995) Chemokine class differences in binding to the Duffy antigen-erythrocyte chemokine receptor. J. Biol. Chem. **270**, 25348–25351
16 Nibbs, R. J. B., Wylie, S. M., Yang, J., Landau, N. L. and Graham, G. J. (1997) Cloning and characterization of a novel promiscuous human beta-chemokine receptor D6. J. Biol. Chem. **272**, 32078–32083
17 Middleton, J., Neil, S., Wintle, J., Clark-Lewis, I., Moore, H., Lam, C., Auer, M., Hub, E. and Rot, A. (1997) Transcytosis and surface presentation of IL-8 by venular endothelial cells. Cell **91**, 385–395
18 Nibbs, R. J. B., Ponath, P. D., Parent, D., Qin, S., Campbell, J. D. M., Henderson, A., Kerjaschki, D., Graham, G. J. and Rot, A. (2001) The beta-chemokine receptor D6 is expressed by lymphatic endothelium and a subset of vascular tumors. Am. J. Pathol. **158**, 867–877
19 Fra, A. M., Locati, M., Otero, K., Sironi, M., Signorelli, P., Massardi, M. L., Gobbi, M., Vecchi, A., Sozzani, S. and Mantovani, A. (2003) Cutting edge: Scavenging of inflammatory CC chemokines by the promiscuous putatively silent chemokine receptor D6. J. Immunol. **170**, 2279–2282
20 Proudfoot, A. E. I. (2002) Chemokine receptors: Multifaceted therapeutic targets. Nat. Rev. Immunol. **2**, 106–115
21 Clapham, P. R. (1997) HIV and chemokines: Ligands sharing cell-surface receptors. Trends Cell Biol. **7**, 264–268
22 Gerard, C. and Rollins, B. J. (2001) Chemokines and disease. Nat. Immunol. **2**, 108–115
23 Muller, A., Homey, B., Soto, H., Ge, N. F., Catron, D., Buchanan, M. E., McClanahan, T., Murphy, E., Yuan, W., Wagner, S. N. et al. (2001) Involvement of chemokine receptors in breast cancer metastasis. Nature (London) **410**, 50–56

24 Jones, D., O'Hara, C., Kraus, M. D., Perez-Atayde, A. R., Shahsafaei, A., Wu, L. J. and Dorfman, D. M. (2000) Expression pattern of T-cell-associated chemokine receptors and their chemokines correlates with specific subtypes of T-cell non-Hodgkin lymphoma. Blood **96**, 685–690
25 Okada, T. and Palczewski, K. (2001) Crystal structure of rhodopsin: implications for vision and beyond. Curr. Opin. Struct. Biol. **11**, 420–426
26 Palczewski, K., Kumasaka, T., Hori, T., Behnke, C. A., Motoshima, H., Fox, B. A., Le Trong, I., Teller, D. C., Okada, T., Stenkamp, R. E. et al. (2000) Crystal structure of rhodopsin: A G protein-coupled receptor. Science **289**, 739–745
27 Fryksdale, B. G., Jedrzejewski, P. T., Wong, D. L., Gaertner, A. L. and Miller, B. S. (2002) Impact of deglycosylation methods on two-dimensional gel electrophoresis and matrix assisted laser desorption/ionization-time of flight-mass spectrometry for proteomic analysis. Electrophoresis **14**, 2184–2193
28 Farzan, M., Mirzabekov, T., Kolchinsky, P., Wyatt, R., Cayabyab, M., Gerard, N. P., Gerard, C., Sodroski, J. and Choe, H. (1999) Tyrosine sulfation of the amino terminus of CCR5 facilitates HIV-1 entry. Cell **96**, 667–676
29 Seibert, C., Cadene, M., Sanfiz, A., Chait, B. T. and Sakmar, T. P. (2002) Tyrosine sulfation of CCR5 N-terminal peptide by tyrosylprotein sulfotransferases 1 and 2 follows a discrete pattern and temporal sequence. Proc. Natl. Acad. Sci. U.S.A. **99**, 11031–11036
30 Mirzabekov, T., Kontos, H., Farzan, M., Marasco, W. and Sodroski, J. (2000) Paramagnetic proteoliposomes containing a pure, native and oriented seven-transmembrane segment protein, CCR5. Nat. Biotechnol. **18**, 649–654
31 David, N. E., Gee, M., Andersen, B., Naider, F., Thorner, J. and Stevens, R. C. (1997) Expression and purification of the Saccharomyces cerevisiae α-factor receptor (Ste2p), a 7-Transmembrane-segment G protein-coupled receptor. J. Biol. Chem. **272**, 15553–15561
32 Ohtaki, T., Ogi, K., Masuda, Y., Mitsuoka, K., Fujiyoshi, Y., Kitada, C., Sawada, H., Onda, H. and Fujino, M. (1998) Expression, purification and recycling of receptor for pituitary adenylate cyclase-activating polypeptide. J. Biol. Chem. **273**, 15464–15473
33 Klassen, C. H. W., Bovee-Geurts, P. H. M., Decaluwe, G. L. J. and Degrip, W. J. (1999) Large-scale production and purification of functional recombinant bovine rhodopsin with the use of the baculovirus expression system. Biochem. J. **342**, 293–300
34 Shimada, M., Chen, X., Cvrk, T., Hilfiker, H., Parfenova, M. and Segre, G. V. (2002) Purification and characterization of a receptor for human parathyroid hormone and parathyroid hormone-related peptide. J. Biol. Chem. **277**, 31774–31780

Received 19 August 2003/23 December 2003; accepted 15 January 2004
Published as BJ Immediate Publication 15 January 2004, DOI 10.1042/BJ20031266

35 Warne, T., Chrinside, J. and Schertler, G. F. X. (2003) Expression and purification of truncated, non-glycosylated turkey beta-adrenergic receptors for crystallization. Biochim. Biophys. Acta **1610**, 133–140
36 Mirzabekov, T., Bannert, N., Frazan, M., Hofmann, W., Kolchinsky, P., Wu, L., Wyatt, R. and Sodroski, J. (1999) Enhanced expression, native purification and characterization of CCR5, a principal HIV-1 coreceptor. J. Biol. Chem. **274**, 28745–28750
37 Babcock, G. J., Mirtzabekov, T., Wojtowicz, W. and Sodroski, J. (2001) Ligand binding characteristics of CXCR4 incorporated into paramagnetic proteoliposomes. J. Biol. Chem. **276**, 38433–38440
38 Borjigin, J. and Nathans, J. (1994) Insertional mutagenesis as a probe of rhodopsin's topography, stability, and activity. J. Biol. Chem. **269**, 14715–14722
39 Sagne, C., Isambert, M.-F., Henry, J.-P. and Gasnier, B. (1996) SDS-resistant aggregation of membrane proteins: application to the purification of the vesicular monoamine transporter. Biochem. J. **316**, 825–831
40 Rodriguez-Frade, J. M., Mellado, M. and Martinez, C. (2001) Chemokine receptor dimerization: two are better than one. Trends Immunol. **22**, 612–617
41 Aramori, I., Zhang, J., Ferguson, S. S. G., Bieniasz, P. D., Cullen, B. R. and Caron, M. G. (1997) Molecular mechanism of desensitization of the chemokine receptor CCR-5: receptor signaling and internalization are dissociable from its role as an HIV-1 co-receptor. EMBO J. **16**, 4606–4616
42 Pollok-Kopp, B., Schwarze, K., Baradari, V. K. and Oppermann, M. (2003) Analysis of ligand-stimulated CC chemokine receptor 5 (CCR5) phosphorylation in intact cells using phosphosite-specific antibodies. J. Biol. Chem. **278**, 2190–2198
43 Mokros, T., Rehm, A., Droese, J., Oppermann, M., Lipp, M. and Hopken, U. E. (2002) Surface expression and endocytosis of the human cytomegalovirus-encoded chemokine receptor US28 is regulated by agonist-independent phosphorylation. J. Biol. Chem. **277**, 45122–45128
44 Fraile-Ramos, A., Kledal, T. N., Pelchen-Matthews, A., Bowers, K., Schwartz, T. W. and Marsh, M. (2001) The human cytomegalovirus US28 protein is located in endocytic vesicles and undergoes constitutive endocytosis and recycling. Mol. Biol. Cell **12**, 1737–1749
45 Venkatesan, S., Rose, J. J., Lodge, R., Murphy, P. M. and Foley, J. F. (2003) Distinct mechanisms of agonist-induced endocytosis for human chemokine receptors CCR5 and CXCR4. Mol. Biol. Cell **14**, 3305–3324